International Journal of High-Rise Buildings
December 2018, Vol 7, No 4, 313-325
https://doi.org/10.21022/IJHRB.2018.7.4.313

International Journal of
High-Rise Buildings
www.ctbuh-korea.org/ijhrb/index.php

Boundary Conditions and Fire Behavior of Concrete Filled Tubular Composite Columns

João Paulo C. Rodrigues[1†], António J. M. Correia[2], and Venkatesh Kodur[3]

[1]*LAETA, Department of Civil Engineering, University of Coimbra, Portugal*
[2]*LAETA, Department of Civil Engineering, Polytechnic Institute of Coimbra, Portugal*
[3]*Department of Civil & Environmental Engineering, Michigan State University, USA*

Abstract

Concrete-filled steel tubular (CFST) members are commonly used as composite columns in modern construction. However, the current guidelines for members' fire design (EN1994-1-2) have been proved to be unsafe in case the relative slenderness is higher than 0.5. In addition, the simplified design methods of Eurocode 4 are limited to circular and square CFST columns, while in practice columns with rectangular and elliptical hollow sections are being increasingly used because of their architectural aesthetics. In the last years a large experimental research has been carried out at Coimbra University on the topic. They have been tested concrete filled circular, square, rectangular and elliptical hollow columns with restrained thermal elongation. Some parameters such as the slenderness, the type of cross-section geometry as well as the axial and rotational restraint of the surrounding structure to the column have been tested in order to evaluate their influence on the fire resistance of such columns. In this paper it is evaluated the influence of the boundary conditions (pin-ended and semi-rigid end-support conditions) on the behavior of the columns in case of fire. In these tests it could not be seen a marked effect of the tested boundary conditions but it is believed that the increasing of rotational stiffness increases the fire resistance of the columns.

Keywords: Fire, Composite, Hollow column, Thermal restraint, Support conditions

0. Notation

CFST	concrete-filled steel tubular
CC	circular column
EC	elliptical column
RC	rectangular column
SC	square column
A	cross-sectional area of the column
A_m/V	section factor
b	short dimension of the cross-section (width of the cross-section)
d	long dimension of the cross-section (length of the cross-section)
L	effective buckling length of a column in the plane of bending
t	wall thickness of steel tube
f_c	compressive strength of the concrete at normal temperature
f_y	yield strength of the steel at normal temperature
ρ_s	longitudinal steel reinforcement ratio
$\bar{\lambda}$	non-dimensional slenderness of the column at normal temperature
$N_{pl,Rd}$	design resistance to axial compression of the composite section
N_{cr}	minimum elastic critical force for flexural buckling of a compression member with semi-rigid end support conditions
$N_{b,Rd}$	design buckling resistance of a compression member
$k_{a,c}$	axial stiffness of the column
$K_{r,c}$	rotational stiffness of the column about the minor axis
P	axial compression force in the column
P_0	initial applied service load on the column
P/P_0	relative axial restraint forces
k_a	axial restraint imposed by a surrounding structure to the thermal elongation of the column
K_r	rotational restraint imposed by a surrounding structure to the rotation of the column ends subjected to fire (about both principal axes)
K_r	rotational restraint imposed by a surrounding structure to the rotation of the column ends subjected to fire (about both principal axes)
$t_{Pmáx}$	time for maximum axial restraint force
t_{cr}	critical time

1. Introduction

Concrete filled steel tubular (CFST) columns are increasingly assuming a greater role in civil construction.

†Corresponding author: João Paulo C. Rodrigues
Tel: +351-239-797-237; Fax: +351-239-797-123
E-mail: jpaulocr@dec.uc.pt

This is due to the combination of some of the best properties of each material, making it structurally advantageous and an efficient solution (Qiu et al., 2017, Yuan et al., 2018). Concrete filling offers an attractive practical solution for providing fire protection to steel hollow columns without any external protection. The fire resistance of concrete-filled steel hollow section columns may be between 50 and 100 minutes, depending on the type of concrete filling (plain concrete, bar-reinforced concrete or steel fiber-reinforced concrete) (Kodur, 1999) whereas the fire resistance of common steel tube columns is less than 30 minutes (Scullion et al., 2011). This improved fire resistance is also due to the composite action between concrete core and steel tube (Wang et al., 2017).

This type of columns has the particularity of the steel tube first expands more than the concrete core, due to the higher temperature and thermal expansion coefficient of the steel, which sustains the serviceability load applied to the column. In the latter stages the steel tube starts to buckle locally, due to the degradation of the mechanical properties at high temperatures and consequent loss of loadbearing capacity, transferring this way the load to the concrete core. Finally, when the concrete core loses its strength, the column as a whole buckle (Espinos et al., 2016). The existing studies on columns made of concrete-filled steel hollow sections at high temperatures addressed the effect of the depth-to-thickness ratio (Espinos et al., 2015), the column slenderness (Mago and Hicks, 2016), the initial applied load level, the load eccentricity (Yao et al., 2016) and the local buckling in the concrete-filled steel tube on their fire resistance. These studies proved that both the simplified calculation model in clause 4.3.5.1 and the method in Annex H of EN 1994-1-2:2005 lead to unsafe predictions for both axially and eccentrically loaded columns (Albero et al., 2016). However, most studies did not take into account the interaction between the column and the surrounding structure and corresponding boundary conditions. The response of these columns when inserted in a building structure is different than when isolated. Both axial and rotational restraints to the thermal elongation of the column, play a role on column's stability, by inducing different forms of interaction between the heated column and the cold adjacent structure. Whereas the axial restraint to thermal elongation of the columns may have a detrimental effect, the rotational restraint may have a beneficial effect on the fire resistance (Ibañez et al., 2016; Rodrigues and Laim, 2017a).

Therefore, with the main purpose of contributing for the development of simplified design methods for the design of these concrete filled tubular composite columns, it is intended to describe in detail in this paper the behavior of CFST columns in fire situation with particular interest on the influence of the boundary conditions (Rodrigues and Laim, 2017a, 2017b).

2. Experimental Tests

2.1. Test Set-up

The experimental set-up is viewed in Fig. 1. A three-dimensional (3D) frame was built, that allowed positioning the testing columns in the center and thus simulating the surrounding structure to the column. With this experimental set-up different axial restraint, k_a could be imposed by the surrounding structure on the CFST columns, however only the one corresponding to 30 kN/mm is considered in this work. The system is also composed by a two-dimensional (2D) frame, in which a hydraulic jack was positioned, to apply the serviceability loads to the columns.

The columns were placed in the center of the 3D restraining frame and tested with semi-rigid and pin-ended support conditions. The columns had at each end a steel plate S355 that fitted directly to the 3D restraining frame (semi-rigid support condition) or to the pinned support (pin-ended support condition). The connection of the column to the supports have been done in both cases by four M24 steel grade 8.8 bolts. The details of the supports are presented in Fig. 2.

Additionally, above the specimen a 3MN compression load cell was placed to monitor the axial restraining forces



Figure 1. General view of the test set-up.

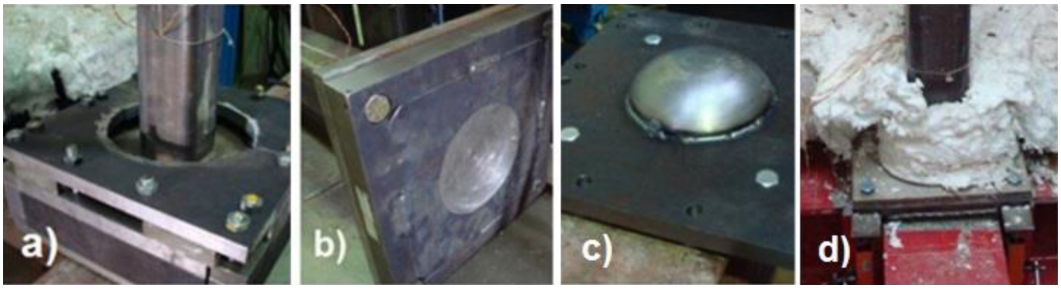


Figure 2. Details of the end supports: (a), (b) and (c) pin-ended; (d) semi-rigid ended.

generated in the CFST columns during the test. The thermal action was applied by a vertical modular electric furnace programmed to reproduce the ISO 834 standard fire curve (ISO 834-1, 1999).

2.2. Tested columns

A great number of experiments on the behavior of concrete filled circular (CC), square (SC), rectangular (RC) and elliptical (EC) hollow columns at high temperatures, was carried out under this experimental program. The specimens were full-scale columns made of hollow steel profiles completely filled with reinforced concrete (Fig. 3), with the mentioned steel cross-sections. All reinforcing bars used in the test specimens were of S500 structural steel and all specimens presented a similar concrete of C25/30 class with calcareous aggregate, according to EN 1992-1-1:2004. In addition, all steel profiles were 3.15 m tall of S355 grade (with a nominal yield strength of 355 MPa and a tensile strength of 510 MPa), according to EN 1993-1-1:2004. Another important point to note is that about five days after concrete casting, the moisture content of the concrete was about 4.5%, according to the procedure described in EN 1097-5:2009. This parameter was measured as soon as possible because the water loss from the concrete inside the steel tubes was too limited.

The following table (Table 1) presents the characteristics of the columns and the calculation of the serviceability loads for the tests carried out. In the last columns of the table, the axial and rotational adimensional stiffness, are also presented. In this paper only the columns tested with axial stiffness of 30 kN/mm were presented the results as the main objective of the paper is to analyse the effect of the boundary conditions on the behaviour of the columns at high temperatures. This stiffness is referenced in the figures by *lka.*

Table 2 presents the dimensions of the steel tubes and the amount of steel rebars adopted in each of the columns used in the experiments. For each specimen the transversal reinforcement was composed of 8 mm diameter stirrups with a spacing of 150 mm until about 800 mm from the supports and with a spacing of 200 mm in the central part. The concrete covering related to the rebars for all tested columns was 25 mm.

For each type of column two different cross-sections were tested, except for the elliptical ones. Therefore, the circular hollow sections were 273 and 193.7 mm with a

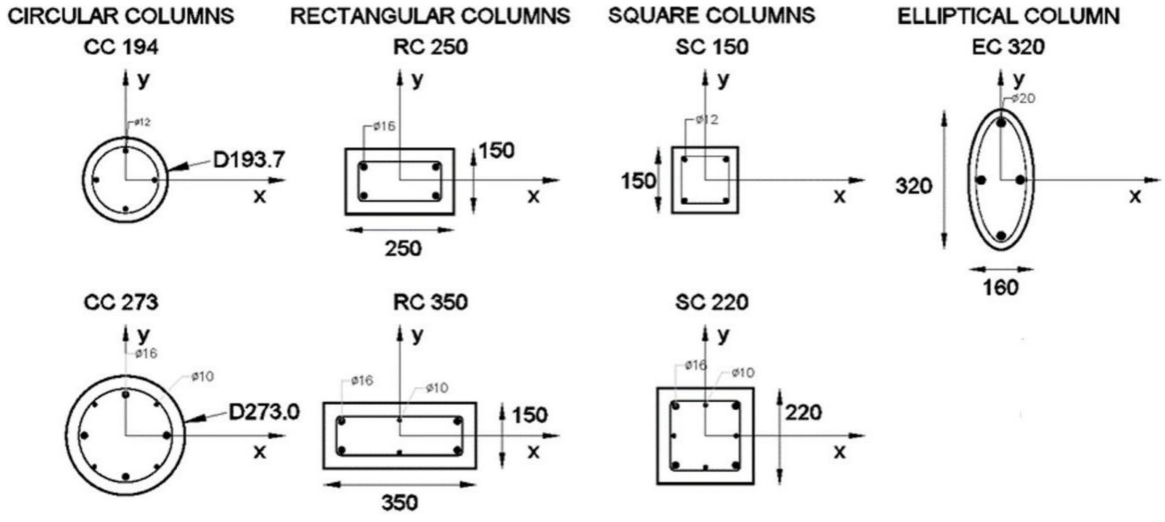


Figure 3. Scheme of the cross-sections of the tested columns.

Table 1. Test programme

Test reference	A (mm^2)	A_m/V (m^{-1})	$\overline{\lambda}$	$N_{pl,Rd}$ (kN)	N_{cr} (kN)	$N_{b,Rd}$ (kN)	$k_{a,c}$ (kN/mm)	$k_{r,c}$ (kN.m/rad)	P_0 (kN)	k_a (kN/mm)	k_r (kN·m/rad)	$k_a/k_{a,c}$	$k_r/(k_r+k_{r,c})$
CC273-30ka-PP	58535	14.7	0.51	4075	17519	3759	1094	24695	1128	30	0	0.03	0
SC220-30ka-PP	48400	18.2	0.54	3987	14562	3627	1005	20528	1088	30	0	0.03	0
CC194-30ka-PP	29468	20.7	0.71	2258	4704	1903	573	6632	571	30	0	0.05	0
RC350-30ka-PP	52500	19.0	0.75	4385	8319	3600	1104	11727	1080	30	0	0.03	0
RC250-30ka-PP	37500	21.3	0.77	3436	6137	2783	837	8651	835	30	0	0.04	0
SC150-30ka-PP	22500	26.7	0.80	2043	3420	1626	500	4820	488	30	0	0.06	0
EC320-30ka-PP	40212	19.8	0.85	4118	6109	2858	965	8612	857	30	0	0.03	0
CC273-30ka-SR	58535	14.7	0.41	4016	26426	3814	1094	24695	1144	30	94615	0.03	0.79
SC220-30ka-SR	48400	18.2	0.44	3987	21967	3751	1005	20528	1125	30	94615	0.03	0.82
CC194-30ka-SR	29468	20.7	0.58	2178	7097	1956	573	6632	587	30	94615	0.05	0.93
RC350-30ka-SR	52500	19.0	0.61	4385	12549	3880	1104	11727	1164	30	94615	0.03	0.89
RC250-30ka-SR	37500	21.3	0.63	3436	9258	3016	837	8651	905	30	94615	0.04	0.92
SC150-30ka-SR	22500	26.7	0.65	2043	5158	1776	500	4820	533	30	94615	0.06	0.95
EC320-30ka-SR	40212	19.8	0.69	4118	9216	3248	965	8612	974	30	94615	0.03	0.92
CC273-110ka-SR	58535	14.7	0.41	4016	26426	3814	1094	24695	1144	110	131340	0.10	0.84
SC220-110ka-SR	48400	18.2	0.44	3987	21967	3751	1005	20528	1125	110	131340	0.11	0.86
CC194-110ka-SR	29468	20.7	0.58	2178	7097	1956	573	6632	587	110	131340	0.19	0.95
RC350-110ka-SR	52500	19.0	0.61	4385	12549	3880	1104	11727	1164	110	131340	0.10	0.92
RC250-110ka-SR	37500	21.3	0.63	3436	9258	3016	837	8651	905	110	131340	0.13	0.94
SC150-110ka-SR	22500	26.7	0.65	2043	5158	1776	500	4820	533	110	131340	0.22	0.96
EC320-110ka-SR	40212	19.8	0.69	4118	9216	3248	965	8612	974	110	131340	0.11	0.94

Table 2. Geometric characteristics of specimens

Test reference	d (mm)	b (mm)	t (mm)	f_y (MPa)	f_c (MPa)	rebars	ρ_s (%)	d/t	d/b
CC273	273.0	-	10.0	365	33	4ϕ16 & 4ϕ10	2.3	27.3	-
CC194	193.7	-	8.0	365	33	4ϕ12	1.9	24.2	-
SC220	220.0	220.0	10.0	410	33	4ϕ16 & 4ϕ10	2.9	22.0	1.0
SC150	150.0	150.0	8.0	410	33	4ϕ12	2.6	18.8	1.0
RC350	350.0	150.0	10.0	420	33	4ϕ16 & 2ϕ10	2.3	35.0	2.3
RC250	250.0	150.0	10.0	420	33	4ϕ16	2.7	25.0	1.7
EC320	320.0	160.0	12.5	375	33	4ϕ20	4.2	25.6	2.0

wall's thickness of 10 and 8 mm (respectively). The square ones were 150 mm and 220 mm wide with a wall's thickness of 10 and 8 mm (respectively). The rectangular ones were 250 mm and 350 mm height and 150 mm wide with a wall's thickness of 10 mm. The elliptical ones had 320 mm height and 160 mm wide with a wall's thickness of 12.5 mm.

The largest circular and square columns had eight longitudinal rebars, four of which were 16 mm in diameter (416) and the other four were 10 mm (4ϕ10). The narrowest column had four longitudinal rebars of 12 mm in diameter (4ϕ12). On the other hand, the largest rectangular column had six longitudinal rebars, four of which of 16 mm in diameter (4ϕ16) and the others of 10 mm (2ϕ 10), whereas the narrowest rectangular column had four longitudinal rebars of 16 mm in diameter (4ϕ16). For the elliptical columns were used 4 rebars of 10 mm in diameter (4ϕ10).

Note that these longitudinal rebars were chosen for this study in order to have similar longitudinal reinforcement ratios between columns with the same geometric shape. As well as that the widest rebars were placed at the corners of the cross-sections and the others in the middle, as shown in Fig. 3 and Table 2.

2.3. Test Procedure

The test procedure first involved the positioning of the CFST test column in the center of the restraining frame, followed by applying the serviceability load. The load level applied on the columns, P_0, was 30% of the design value of the buckling load of the columns at ambient temperature, calculated in accordance with the methods proposed in EN 1994-1-1:2004 (i.e., based on characteristic material properties). During the application of the

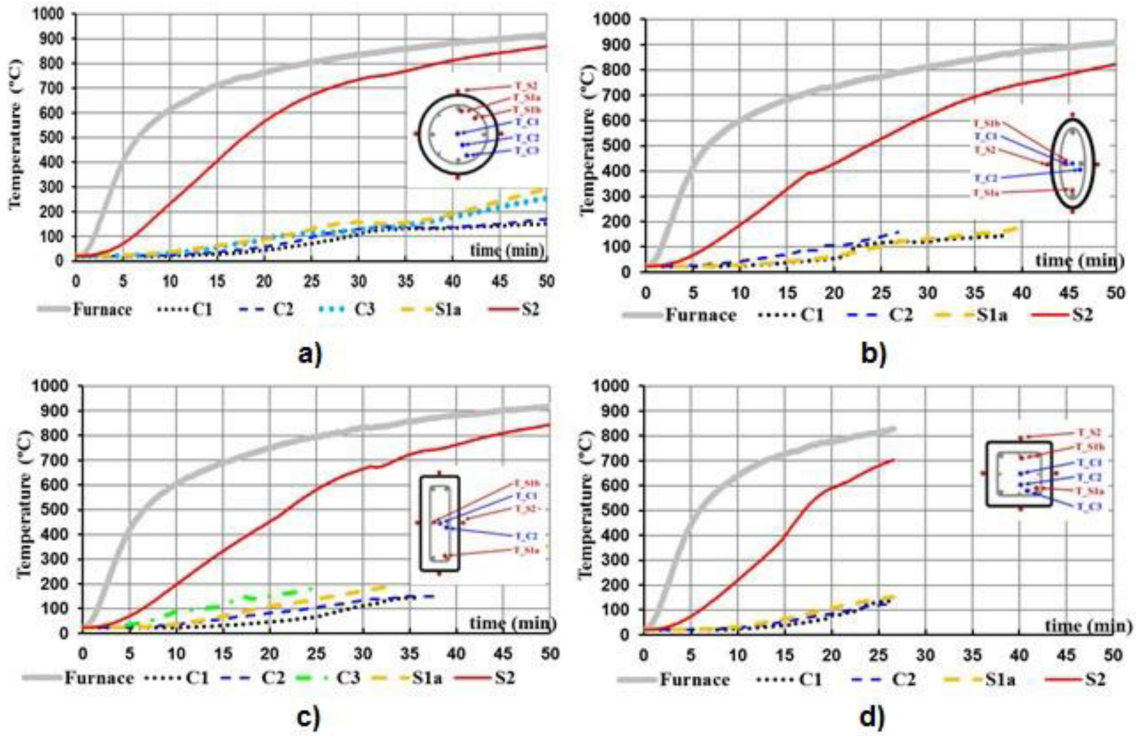


Figure 4. Temperatures at column's mid-height a) CC194-lka-sr, b) EC320-lka-sr, c) RC250-lka-sr and d) SC150-lka-sr.

load, the upper beams of the restraining frame were not connected to the columns in such a way that they could move freely downwards, ensuring that the load was directly applied to the test specimen. Once the predefined load level was reached, the vertical movement of the upper beams of the restraining frame was blocked (the connections between the upper beams and the peripheral columns of the restraining frame were fastened with locking nuts, washers and threaded rods) in order to activate the restraint imposed by the restraining frame on the CFST column. Finally, the electric furnace was turned on, and the specimen was uniformly exposed to the ISO 834 standard fire curve (ISO 834-1, 1999). During the heating period, the load was kept constant until the specimen failed. The failure criterion adopted in this study was based on the ultimate load bearing capacity of the column, that is when it could no longer support the initial applied load (serviceability load).

3. Results

3.1. Temperatures

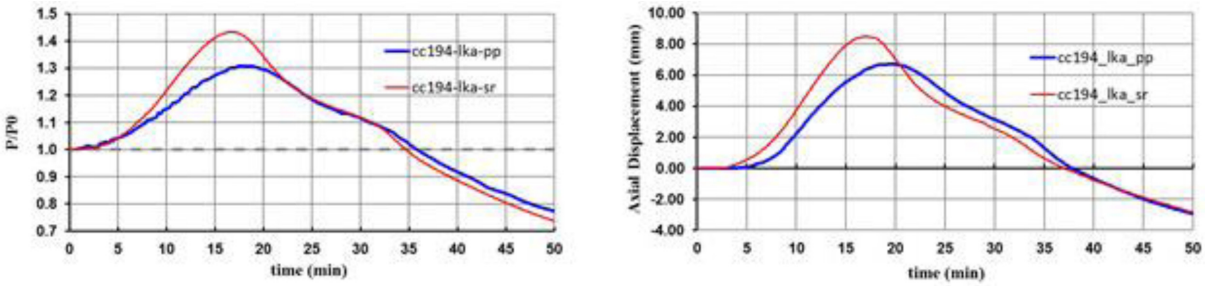
Fig. 4 depicts, as an example, the evolution of temperatures on columns CC194-lka-sr (a), EC320-lka-sr (b), RC 250-lka-sr (c) and SC150-lka-sr (d), as a function of time. All the temperatures presented were measured at mid-height of the columns. For all cases, the lowest axial stiffness, and semi-rigid boundary conditions were chosen. It is possible to observe a great difference of temperatures, between the thermocouples in the concrete and the steel, on the surface outside the columns. Thermocouples named with the letter S, stand for thermocouples in the steel surface, and the letter C stands for the ones inside the concrete. Thermocouple S1 is placed in the steel reinforcement of the column and thermocouple S2 is outside the column.

The temperatures in the steel tube increased faster, trying to accompany the furnace heating curve, while the temperatures in the rebars and concrete increased slower reaching temperatures of not more than 200ºC. A huge difference between the outer surface of steel, and the temperatures inside the concrete, and the reinforcement, was observed. For this temperature level the mechanical properties of the concrete and rebars remain unaffected and indicates that buckling was governed by the external steel tube.

3.2. Restraining forces and axial displacements

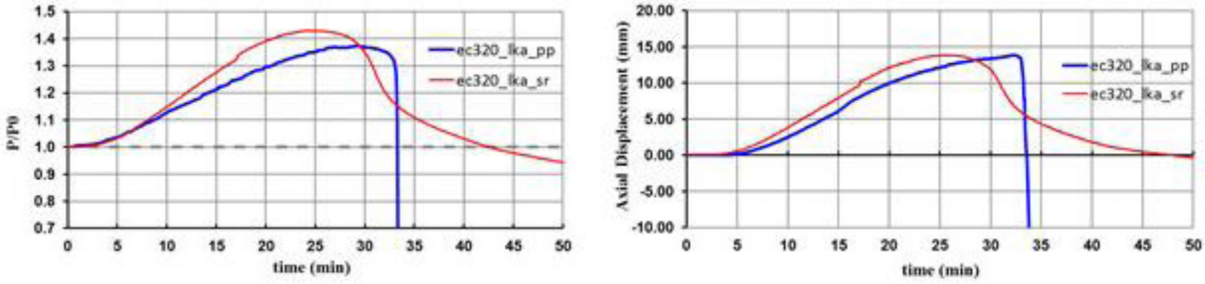
In this section, the evolution of the relative axial forces and vertical displacements in the columns are depicted, in different graphs. In each graph, two different lines are depicted, the red line stands for the semi-rigid boundary condition and the blue line stand for the pin-ended columns. The restraining forces showed the typical behavior of increasing up to a maximum and at a certain point start decreasing, due to degradation of the mechanical properties of the materials with the temperature, reaching again the value of the initial applied loading.

In Fig. 5, the results for the circular column CC-194



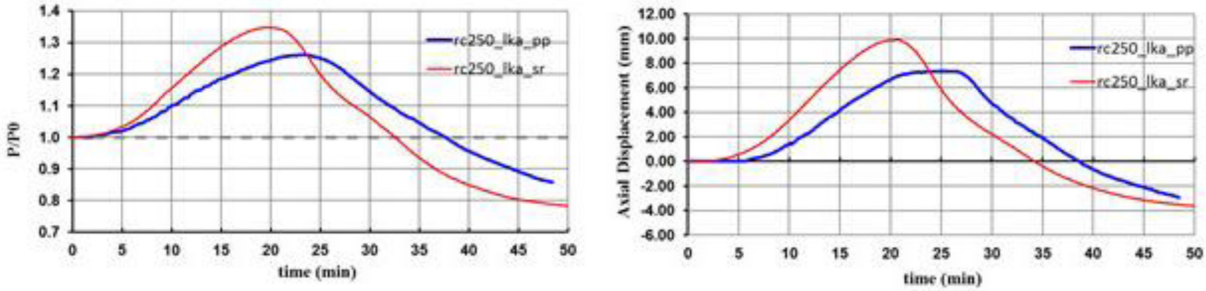
(a) (b)

Figure 5. a) Relative Axial Restraint Force and b) Axial Displacements for column CC194-lka, for semi-rigid and pin-ended boundary conditions.



(a) (b)

Figure 6. a) Relative Axial Restraining Forces and b) Axial Displacements for column EC320-lka for semi-rigid and pin-ended boundary conditions.



(a) (b)

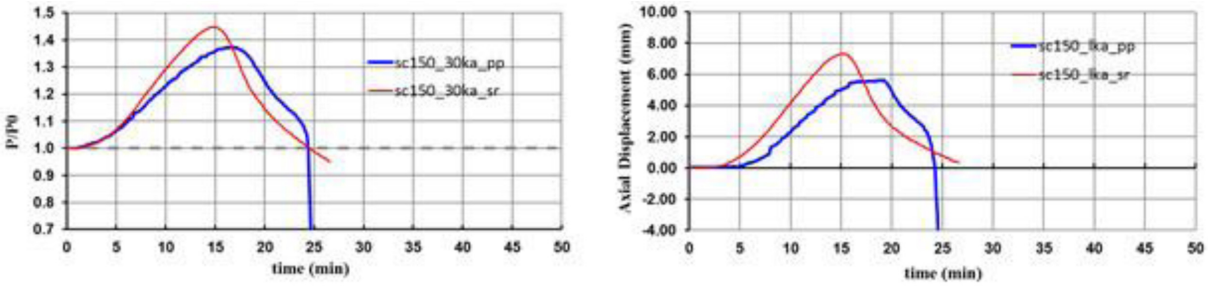
Figure 7. a) Relative Axial Restraining Forces and b) Axial Displacements for column RC250-lka for semi-rigid and pin-ended boundary.

show no major differences between the two boundary conditions, neither for the relative axial forces, neither for the vertical displacements.

In Fig. 6, the results for the elliptical column EC-320 show important differences between the two boundary conditions. The pin-ended column experienced a typical behavior of these columns under fire, with an abrupt decay of the relative restraint forces, and the semi-rigid column presents a gentle decay of the restraining forces. This post-buckling behavior is important in terms of the analysis of the global behavior of the whole structure. It is very different the behavior of a structure with columns suffering an instantaneous loss than with columns suffering smooth a decay of the of load bearing capacity.

In Fig. 7, the results for the rectangular column RC-250 are presented. Despite of the difference in the critical times, with higher resistance presented by the pin-ended, explained maybe by higher local buckling on the semi-rigid columns, the shape of the graphs is pretty much the same.

In Fig. 8, the results for the square columns SC150, show negligible differences on the critical times for both end support conditions. The experimental tests on the pin-ended columns, showed a sudden decay on the restraining forces after the peak value followed by a sudden decay



(a) (b)

Figure 8. a) Relative Axial Restraining Forces and b) Axial Displacements for column SC150-lka for cases of semi-rigid and pin-ended boundary.

Table 3. Maximum relative axial restraining forces, time for the maximum axial restraining forces and critical times

Columns	pined-pined end support			Columns	semi-rigid end support		
	P/P_0	$t_{Pmáx}$ (min.)	t_{cr} (min.)		P/P_0	$t_{Pmáx}$ (min.)	t_{cr} (min.)
CC194-30ka-PP	1.31	17.32	35.7	CC194-30ka-SR	1.43	15.70	34.58
EC320-30ka-PP	1.37	26.20	33.30	EC320-30ka-SR	1.43	23.33	42.13
RC250-30ka-PP	1.26	21.27	37.35	RC250-30ka-SR	1.35	18.88	32.37
SC150-30ka-PP	1.37	15.28	24.42	SC150-30ka-SR	1.45	14.43	24.37

for later stages of the tests and near de critical time.

In general, it can be said that columns with regular cross-sections, with two similar buckling axes, it is not observed any influence of the boundary conditions. On the other hand, columns with two distinct buckling axes, the ones with pin-ended support conditions showed abrupt buckling that occurs around the weak buckling axis.

Table 3 presents the main results of the tests under study: maximum relative axial forces, times from the beginning of the tests and critical times. It is interesting to note that the maximum relative axial restraining forces are greater for the cases on semi-rigid ended support conditions than for pin-ended support conditions. Moreover, except for the elliptical columns, this peak of maximum axial restraining forces, occurred approximately at mid-time of the tests. Only for this type of columns, the semi-rigid ended support conditions provided greater critical time, but it is worth to note that this Table do not reflect the post-buckling behavior of the columns.

3.3. Lateral Deflections and Stiffness of the System

Figs. 9 to 12 depict the deformed shapes of the columns, in the end of the tests, meaning, in the moment considered the collapse of the element. The deformed shapes are drawn around minor and major axis, for each column, elliptical, circular, rectangular and square, for both boundary conditions adopted in the study, pin-ended (*pp*) and semi-rigid (*sr*). In general, as expected, greater deflections were observed for deflections around minor axis, and for double-symmetric cross-sections no important differences were noticed.

Fig. 9 depicts the deformed shapes on the circular columns CC194. It is observed for this column, that the semi-rigid end support conditions provide lower deflections, around both axes. All graphs were plotted for the critical times of 35 minutes, equal for both end conditions.

Fig. 10 depicts the deformed shapes on the elliptical columns EC320. It must be stated that these deformed shapes were plotted for different times, which were considered the critical times for each test. Thus, the pin-ended column has a critical time of 33 minutes and the semi-rigid column has a critical time of 42 minutes meaning that the deformed shapes of Fig. 10 are for different instants of time.

Fig. 11 depicts the deformed shapes on the rectangular columns RC250. In this case a strange result was obtained. The pin-ended column presented a greater critical time than the semi-rigid end condition column. This result was not expectable at all, and may be explained by the strong local buckling observed in this case.

In Fig. 12, the deformed shapes on the square columns SC150 is depicted. In this case, as observed in the circular column, the critical time is almost the same for both end conditions.

Figs. 13 to 16, depict the stiffness of the set, composed by the column and the surrounding frame, for the different types of columns.

In Fig. 13, for the circular column CC194, the stiffness for the case of the pin-ended column was 20.8 kN/mm, and for the case of semi-rigid boundary condition was 31.5 kN/mm.

In Fig. 14, for the elliptical column EC320, the stiffness

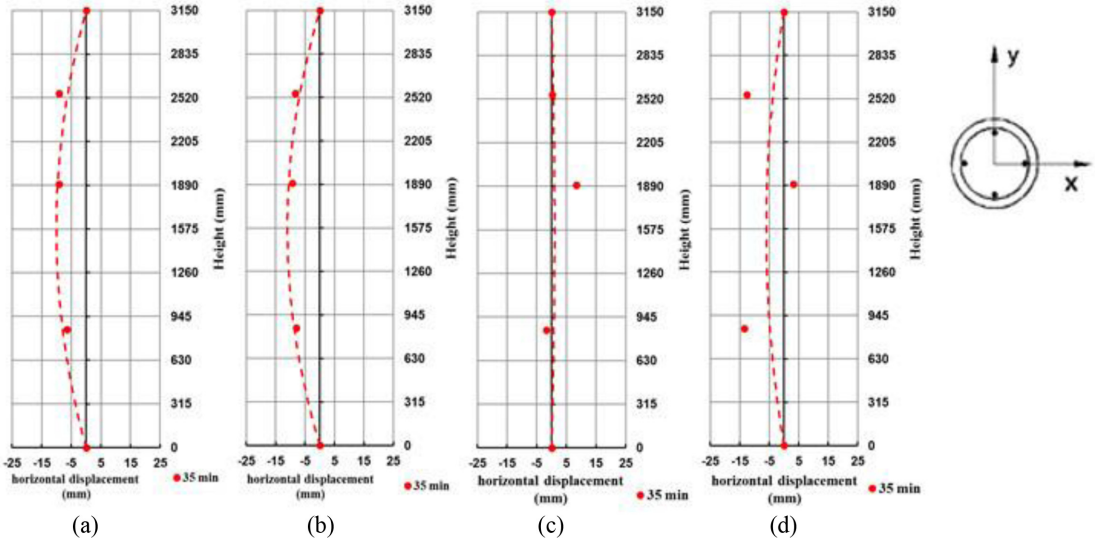


Figure 9. Lateral deflections for columns CC194-lka: a) pp-y axis; b) pp-x axis; c) sr-y axis; d) sr-x axis.

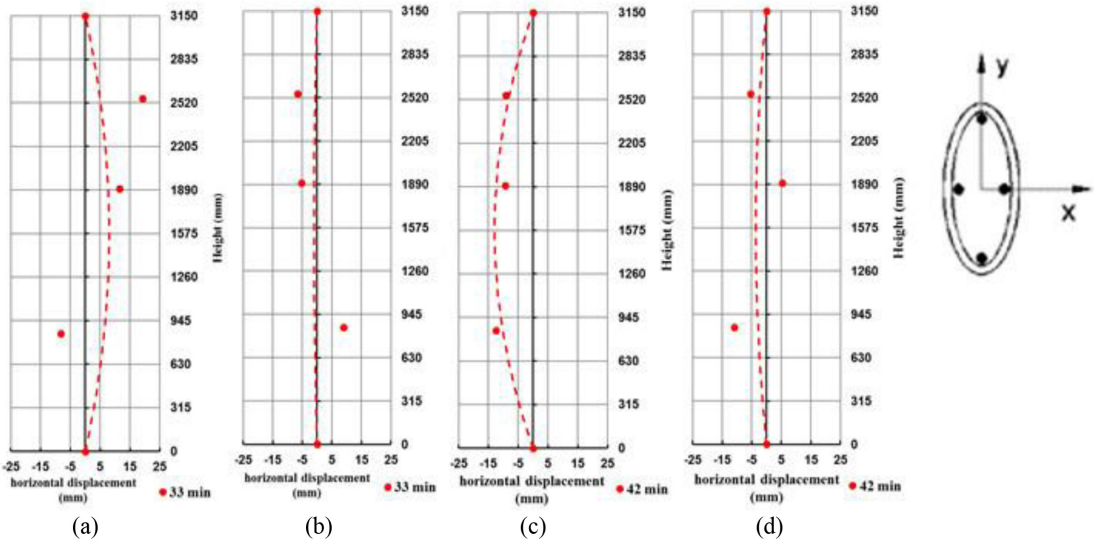


Figure 10. Lateral deflections for column EC320-lka: a) pp-y axis; b) pp-x axis; c) sr-y axis; d) sr-x axis.

was 20.2 kN/mm for the pin-ended, and 29.5 kN/mm for the semi-rigid boundary conditions.

In Fig. 15, for the rectangular column RC250, the values were a little bit higher: 23.3 kN/mm for the pin-ended, and 34.7 kN/mm for the semi-rigid boundary conditions.

In Fig. 16, the lowest values observed were for the square columns: 19.5 kN/mm for the pin-ended column, and 31.1 kN/mm for the semi-rigid column.

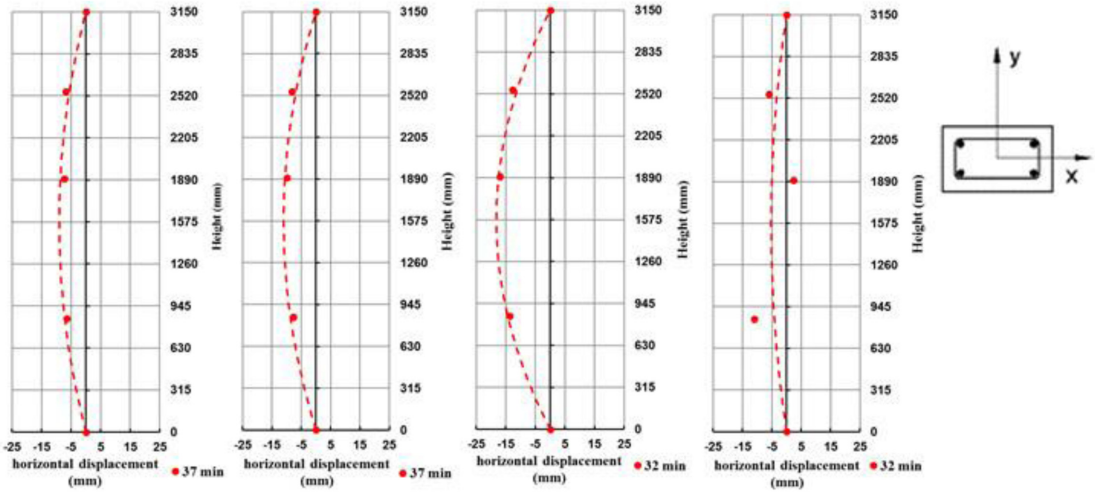
As expected, in all cases the global stiffness was always higher for the case of the semi-rigid connections.

3.4. Rotations

Figs. 17 to 20 depict the rotations on the top of the columns. These rotations were registered with four displacement transducers (three were enough) placed in the corners of the top end plates of the columns and with this allowing determining all rotation planes. With the results of these LVDT´s, it was possible to define the position of the plane defined by the end plate, and its rotation around x and y axis. Fig. 17 depicts the rotations for the circular column CC194.

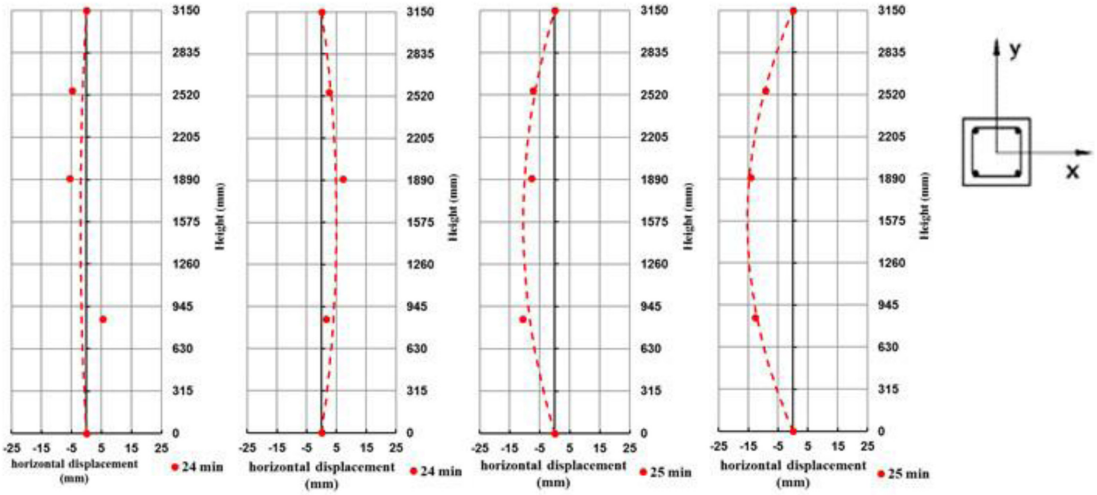
In Fig. 18, the rotations for the elliptical column EC320 are presented. It is clear that the rotations for the semi-rigid support connection were almost negligible, and in the pin-ended column, the rotations around y axis are greater than the ones around x axis.

In Fig. 19, the case of the rectangular column RC250 is showed. Again, the rotations for the semi-rigid connection



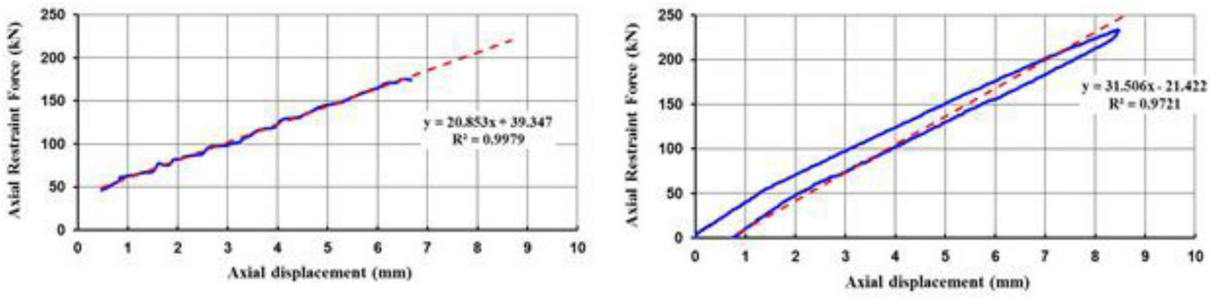
(a) (b) (c) (d)

Figure 11. Lateral deflections for column RC250-lka: a) pp-y axis; b) pp-x axis; c) sr-y axis; d) sr-x axis.



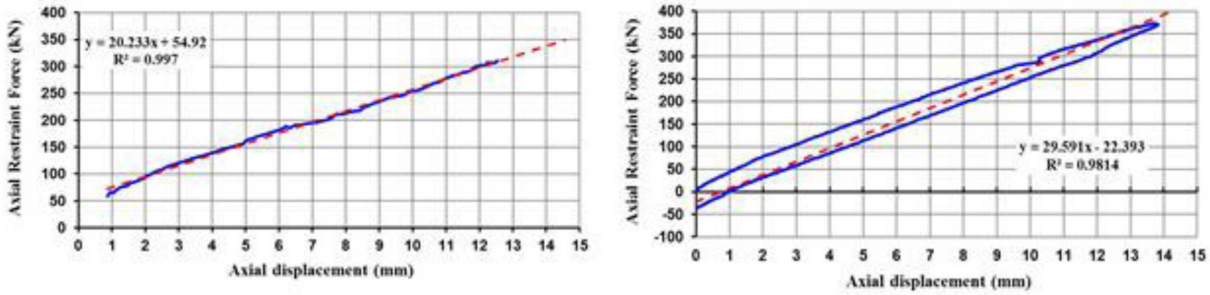
(a) (b) (c) (d)

Figure 12. Lateral deflections for column SC150-lka: a) pp-y axis; b) pp-x axis; c) sr-y axis; d) sr-x axis.



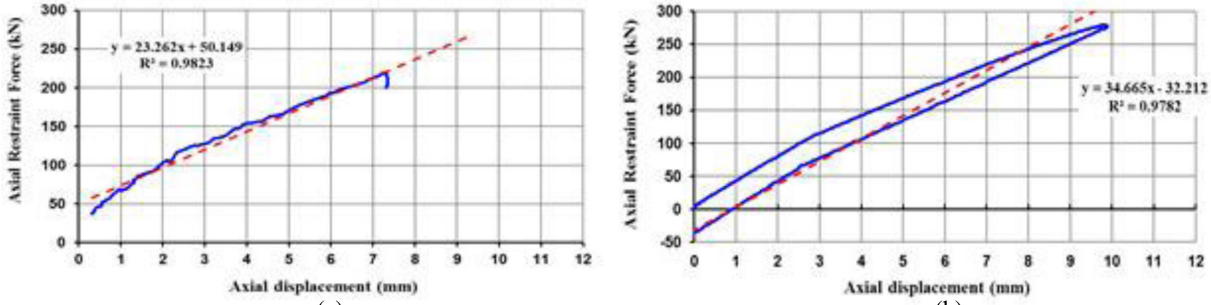
(a) (b)

Figure 13. Stiffness of column CC194-lka for a) pin-ended and b) semi-rigid boundary conditions.



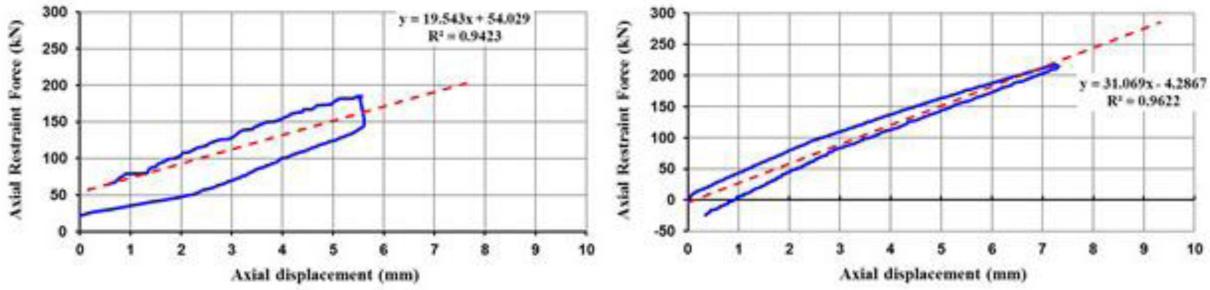
(a) (b)

Figure 14. Stiffness of column EC320-lka for a) pin-ended and b) semi-rigid boundary conditions.



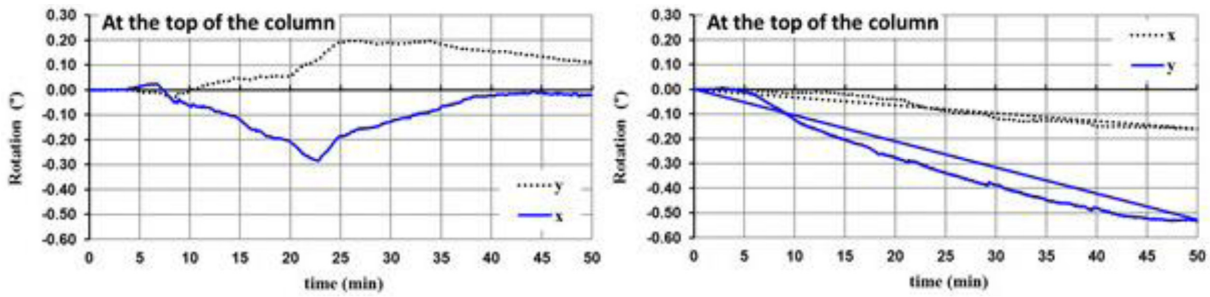
(a) (b)

Figure 15. Stiffness of column RC250-lka for a) pin-ended and b) semi-rigid boundary conditions.



(a) (b)

Figure 16. Stiffness of column SC150-lka for a) pin-ended and b) semi-rigid boundary conditions.



(a) (b)

Figure 17. Rotations on top of column CC194-lka for a) pin-ended and b) semi-rigid boundary conditions.

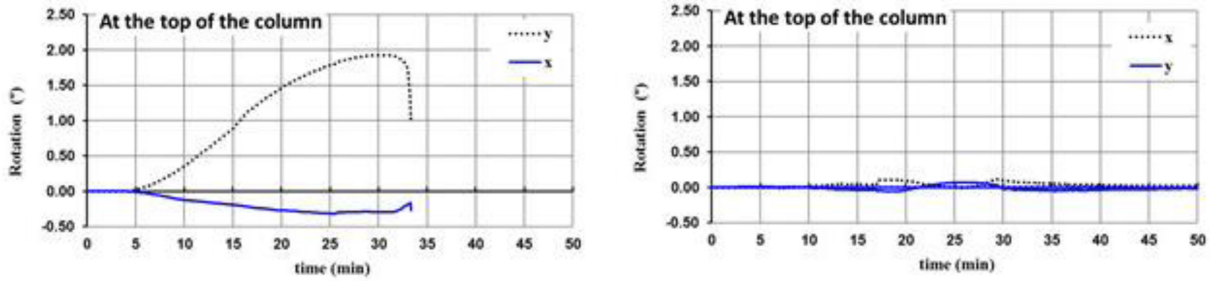


Figure 18. Rotations on top of column EC320-lka for a) pin-ended and b) semi-rigid boundary conditions.

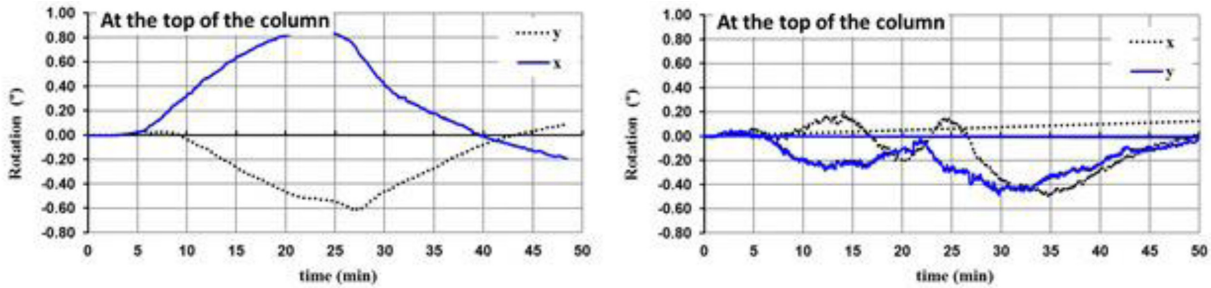


Figure 19. Rotations on top of column RC250-lka for a) pin-ended and b) semi-rigid boundary conditions.

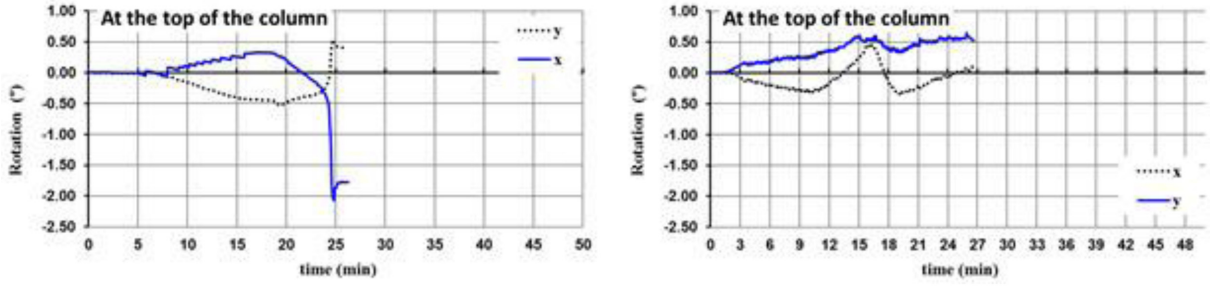


Figure 20. Rotations on top of column SC150-lka for a) pin-ended and b) semi-rigid boundary conditions.

were very low, and for the pin-ended column the rotations around the minor axis are greater than the ones around major axis, as expected.

Fig. 20, depicts the case of the square column RC150. Again, the rotations for the semi-rigid connection were very low, and for the pin-ended column the rotations around x axis suffer an abrupt increase, which may be explained by some geometrical imperfections of the column, or some initial eccentricities. However, this abrupt behavior is congruent with the abrupt decay of the relative axial restraining forces and also the axial displacement.

3.5. Deformed Shapes after test

Fig. 21 shows the deformed shapes of the columns after fire tests concerning to the pin-ended support conditions for the four different cross-sections studied. It may be observed by these Figures that the columns with pin-ended boundary conditions present a more pronounced deformed shape than the columns with semi-rigid connections.

Fig. 22 shows the columns after the fire tests with semi-rigid boundary conditions. In these cases, the deformed shapes by the end of the experimental tests are very smooth.

In Fig. 23 some rectangular and square columns are shown. In these Figures it may be observed the local buckling in some parts of the columns, mainly in the bottom half, which may be the reason of some premature failure of the columns. This local buckling was only observed in



Figure 21. Columns after fire test a) CC194-lka-pp; b) EC320-lka-pp; c) RC250-lka-pp; d) SC150-lka-pp.

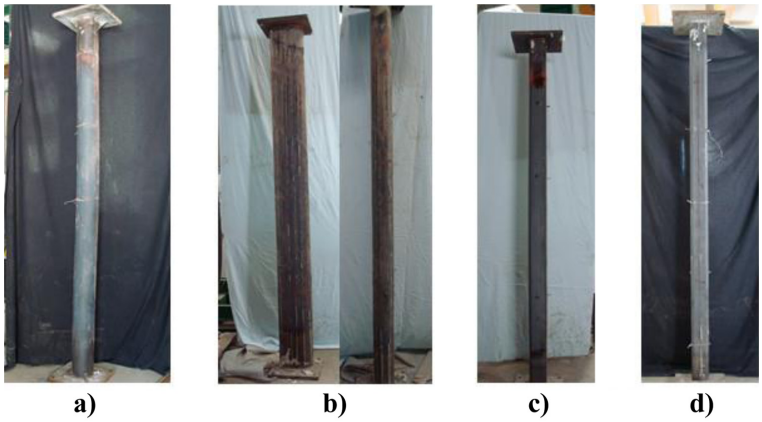


Figure 22. Columns after fire test a) CC194-lka-sr; b) EC320-lka-sr; c) RC250-lka-sr; d) SC150-lka-sr.



Figure 23. Deformed shapes of rectangular and square columns showing local buckling of steel profile.

square and rectangular cross-sections. This phenomenon is a detrimental detail in the fire resistance of the reinforced concrete filled steel composite columns.

4. Conclusions

The main purpose of this research was to provide data for assessing the fire resistance of the concrete filled

hollow columns. The advantages of this type of columns are widely known, especially in fire situation, with the steel tube providing confinement to the concrete and thus preventing its spalling and the concrete inside the tube preventing the loss of structural integrity of the steel for the high temperatures.

The adoption of elliptical columns, as the ones used in the present study is very interesting from the aesthetic point of view. However, as they have two well-defined buckling axes sudden collapse around the weak axis was observed especially for the pin-ended columns.

Comparing the rectangular with the square columns, the first ones presented a greater fire resistance, despite the fact that they were tested with a bigger cross-section. Comparing the elliptical with the circular columns, the elliptical only presented greater fire resistance for the semi-rigid boundary conditions. For the pin-ended columns, the elliptical presented a poor fire performance, comparing with the circular ones. Again, it must be noted that different cross-section dimensions are being compared.

The quantitative results of this research project are valuable to provide data for future numerical studies with focus on parametric analysis of the behaviour of these solutions under fire situation. Interesting outcomes were obtained, as the post-buckling of some columns, the rotations of the pinned-ended and semi-rigid columns, the stiffness of the set column-frame showing expected values for all cases. Further development of this research, with the results of these tests, numerical models will be calibrated, and detailed numerical models will provide data for fire design of these elements.

Acknowledgements

The authors gratefully acknowledge to the EU Research Fund for Coal and Steel (RFCS) for its support under the framework of the research project RFSRCT-2012-00025.

References

Albero V., Espinos A., Romero M. L., Hospitaler A., Bihina G., Renaud C. (2016). *Proposal of a new method in EN1994-1-2 for the fire design of concrete filled steel tubular columns*. Engineering Structures 128: 237–255.

EN 1097-5 (2009). Test for mechanical and physical properties of aggregates – Part 5: Determination of the water content by drying in a ventilated oven. European Committee for Standardization. Brussels, Belgium.

EN 1992-1-1 (2004). Eurocode 2 - Design of concrete structures - Part 1-1: General rules and rules for buildings. European Committee for Standardization. Brussels, Belgium.

EN 1993-1.1 (2004). Design of steel structures. General rules and rules for buildings. European Committee for Standardization. Brussels, Belgium.

EN 1994-1-1 (2004). Eurocode 4 - Design of composite steel and concrete structures - Part 1-1: General rules and rules for buildings. European Committee for Standardization. Brussels, Belgium.

EN 1994-1-2 (2005). Eurocode 4 - Design of composite steel and concrete structures, Part 1-2: General rules - Structural fire design. European Committee for Standardization. Brussels, Belgium.

Espinos A., Romero M. L., Lam D. (2016). *Fire performance of innovative steel-concrete composite columns using high strength steels*. Thin-Walled Structures 106: 113–128.

Espinos A., Romero M. L., Serra E., Hospitaler A. (2015). *Experimental investigation on the fire behaviour of rectangular and elliptical slender concrete-filled tubular columns*. Thin-Walled Structures 93: 137-148.

Ibañez C., Romero M. L., Hospitaler A. (2016). *Effects of axial and rotational restraints on concrete-filled tubular columns under fire*. Jour. Constr. Steel Research 125: 114–127.

ISO 834-1 (1999) Fire resistance tests – elements of building construction, Part 1: general requirements, International Organization for Standardization, Geneva, Switzerland.

Kodur V. (1999). *Performance-based fire resistance design of concrete-filled steel columns*. Journal of Constructional Steel Research 51: 21-36.

Mago N., Hicks S. J. (2016). *Fire behaviour of slender, highly utilized, eccentrically loaded concrete filled tubular columns*. Journal of Constructional Steel Research 119: 123–132.

Qiu W., McCann F., Espinos A., Romero M. L., Gardner L. (2017). *Numerical analysis and design of slender concrete-filled elliptical hollow section columns and beam-columns*. Engineering Structures 131: 90–100.

Rodrigues J. P. C., Laím L. (2017a). *Fire response of restrained composite columns made with concrete filled hollow sections under different end-support conditions*. Eng. Structures 141: 83-96.

Rodrigues J. P. C., Laím L. (2017b). *Fire resistance of restrained composite columns made of concrete filled hollow sections*. Journal of Constructional Steel Research 133: 65-76.

Scullion T., Ali F., Nadjai A. (2011). *Effect of axial restraint on the performance of Elliptical Hollow Section steel columns, in hydrocarbon fire*. Engineering Structures 33: 3155–3161.

Wang Y., Chen P., Liu C., Zhang Y. (2017). *Size effect of circular concrete-filled steel tubular short columns subjected to axial compression*. Thin-Walled Structures 120: 397–407.

Yao Y., Li H., Guo H., Tan K. (2016). *Fire resistance of eccentrically loaded slender concrete-filled steel tubular columns*. Thin-Walled Structures 106: 102-112.

Yuan F., Chen M., Huang H., Xie L., Wang C. (2018). *Circular concrete filled steel tubular (CFST) columns under cyclic load and acid rain at-tack: Test simulation*. Thin-Walled Struct. 122: 90–101.